Studying Properties of RNA Nanotubes via Molecular Dynamics

Badu, S., Melnik, R., and Prabhakar, S.

Studying Properties of RNA Nanotubes via Molecular Dynamics

Shyam Badu; Roderick Melnik and Sanjay Prabhakar

MS2Discovery Interdisciplinary Research Institute, M ^{2}NeT Laboratory, Wilfrid Laurier University, Waterloo, ON, N2L 3C5 Canada;

ABSTRACT

RNA molecules are very flexible in nature. This feature allows us to build various motifs which are essential in bio-nanotechnological applications. Based on our earlier developed models of RNA nanoclusters, in this contribution we analyze the structure and properties of RNA nanotubes in physiological solutions at different concentrations. Our major tool here is the molecular dynamics (MD) method that was implemented by using the NAMD and VMD packages, with which we study the structural and thermal properties of the nanotubes in physiological solutions. In particular, we have analyzed such characteristics as the Root Mean Square Deviation (RMSD), the radius of gyration, the number of hydrogen bonds per base pairs, and the radial distribution function (RDF) of a RNA nanotube at different concentrations of the physiological solution. Furthermore, the number of ^{23}Na$^+$and ^{35}Cl$^-$ions around the nanotubes within the distance of 5 Å at two different concentrations has also been analyzed in detail. It has been found that the number of ions accumulated around the nanotubes within the particular distance is growing by small amount while the concentrations of the ^{23}Na$^+$and ^{35}Cl$^-$ions are substantially increased.

Keywords: RNA Nanotube, Nanobiotechnology, Physiological Solution, Molecular Dynamics Simulation.

1. INTRODUCTION

The structural nature of the RNA nanotube makes it to be very useful for many current and potential applications. The important feature of the RNA nanoclusters is that they are superior to the DNA self-assembled nanoclusters due to their low free energy.[1,2] Today, the nucleic acid nanotechnology research attracts increasing attention in biomedical and bioengineering applications[3,4]. For these applications it is very important to built the proper self assembly of the RNA building blocks. Among many achievements in the field, one of the important nanostructures that has been built is the bacteriophage ϕ 29 motor that can be used to package the DNA. We note that the experimental process for combining the DNA molecules have also been studied[5]. To construct any kind of nanostructure involving biomolecules the self assembly of small building blocks is very important. RNA has been used to build the higher order self assembly in vitro[6] and in vivo[7] by assembling the multidimensional RNA structures. Using the RNAI/II building blocks the structures of the RNA nanoclusters have been constructed in the earlier works.[8–10] The building blocks of these RNA nanoclusters i.e the RNAI and RNAII are defined as the sense and anti sense plasmids that control the replication of COLE1.[11,12] COLE1 is a DNA molecule separated from chromosomal DNA that is found in the cell of bacteria. The sequences for the RNAI is (GGCAACGGAUGGUUCGU-UGCC) and that for the RNAII is (GCACCGAACCAUCCGGUGC).[13]

We note that an experimental study of the concentration dependence of NaCl and KCl on free energy of RNA hairpin folding has been reported earlier.[14] The ionic concentration dependence studies on the binding of HIV -B virus has also been studied and it has been found that the binding of two human immunodeficiency viruses type-1 (HIV-1) is much more favourable at high concentration of salt in the presence of magnesium ion.[15,16] Furthermore, the dependence of the self assembly of the tecto RNA has also attracted interest.[15] These studies motivate to perform more systematic computational studies that can shed further light on the properties of RNA nanoclusters depending on the concentration of the salt solution. This can be done with molecular dynamics simulations. Therefore, in our current study the calculation of the properties has been performed at the concentration where the number of ^{23}Na$^+$and ^{35}Cl$^-$ions is equal to the number of residue i.e the number of phosphate groups in the entire RNA nanotube. Here we built the RNA nanotubes from the piles of RNA nanorings which are the self assembled structures of six segments of RNAI/RNAII complex . The starting structures of the RNAIi/RNAIIi complex are taken from the protein data bank with the pdb code (2bj2.pdb).[13]

The rest of this paper is organized as follows. In section 2 we describe the computational methodologies used for calculations. The results are presented and discussed in Section 3. Concluding remarks and an outlook are then stated in Section 4.

2. COMPUTATIONAL DETAILS

In the modern development of the computational methods, the classical Molecular Dynamics simulation is one of the most versatile tools for the modeling of biological systems.[17,18] In our current study the modeling, including the process of solvation and the ionization of the RNA nanotube, has been carried out by using VMD. In order to perform the molecular dynamics simulation we used the CHARMM27 force field[19] implemented by the software package NAMD.[20] In the molecular dynamics simulation the classical equations of motion of a molecular system are solved by their time dependent integration. The potential of the system used during the molecular dynamics simulation using CHARMM force filed can be expressed as follows:

$$V_{total} = \sum_{bond} K_b (r - r_0)^2 + \sum_{angle} K_\theta (\theta - \theta_0)^2 + \sum_{dihedral} K_\phi (1 + cos(n\phi - \gamma))$$
$$+ \sum_{Hbond} (\frac{C_{ij}}{r_{ij}^{12}} - \frac{D_{ij}}{r_{ij}^{10}}) + \sum_{Vanderwaals} (\frac{A_{ij}}{r_{ij}^{12}} - \frac{B_{ij}}{r_{ij}^{10}}) + \sum \frac{q_{ij}}{\varepsilon r_{ij}} \tag{1}$$

where the first term corresponds to bonds, second corresponding to angle parameters and so on as indicated in the Equation 1 defining the potential of the system. From the above expression for the total potential energy of the system, it is clear that the energy is a function of the positions of particles. If the position of the particle at a time t is known, then its value after the time step δt i.e $t + \delta t$ can be calculated by using the Taylor series expansion as follows:

$$x(t) = x_0 + v_0 t + a_0 \frac{t^2}{2}......, \tag{2}$$

$$x(t + \delta t) = x(t) + v(t)\delta t + \frac{F(t)}{m} \frac{\delta t^2}{2}...... \tag{3}$$

The velocity of an atom at time t and $t + \delta t$ can also be calculated using the acceleration of the atom, similar to the way how the position is calculated from the velocity based on Equations 2 and 3. From the potential energy of the system the acceleration of the kth particle can also be calculated from the Newton's equation of motion as

$$a_k(t) = -\frac{1}{m} \frac{dV_{total}}{dr_k(t)}. \tag{4}$$

Alternatively, the force of an atom during MD simulation can be expressed as

$$F_k(t) = m_k \frac{d^2 r_k(t)}{dt^2} = \frac{dV}{dr}, \tag{5}$$

where the $r_k(t)$ is characterised by the coordinates $(x_k(t), y_k(t), z_k(t))$ in three dimensions.

The output of the molecular dynamics simulation has also been analysed by using VMD to calculate the radial distribution, ion distribution, RMSD and the radius of gyration at different concentrations of salt solution. The RNA-nanotube modeled from the RNA building blocks has been solvated in a water box. The size of the box is taken in such a way that the distance from the surface of nanocluster to the wall is slightly larger than the cut off radius used in the MD simulation. In order to make the system neutral we have added 924 $^{23}Na^+$ to the nanotubes. On top of this, before the MD simulation the RNA nanotube with three nanorings is ionized with the 924, 1848, and the 2772 $^{23}Na^+$ and $^{35}Cl^-$ ions to change the ionic concentration in the MD simulation system. This system was first simulated at constant temperature and pressure using NAMD software. The temperature in the system has been controlled by using Langevin's method with damping parameter $\eta = 5$ ps^{-1}. For adding chemical bonds between the segments in the nanoclusters we have used the topotools available in the VMD.
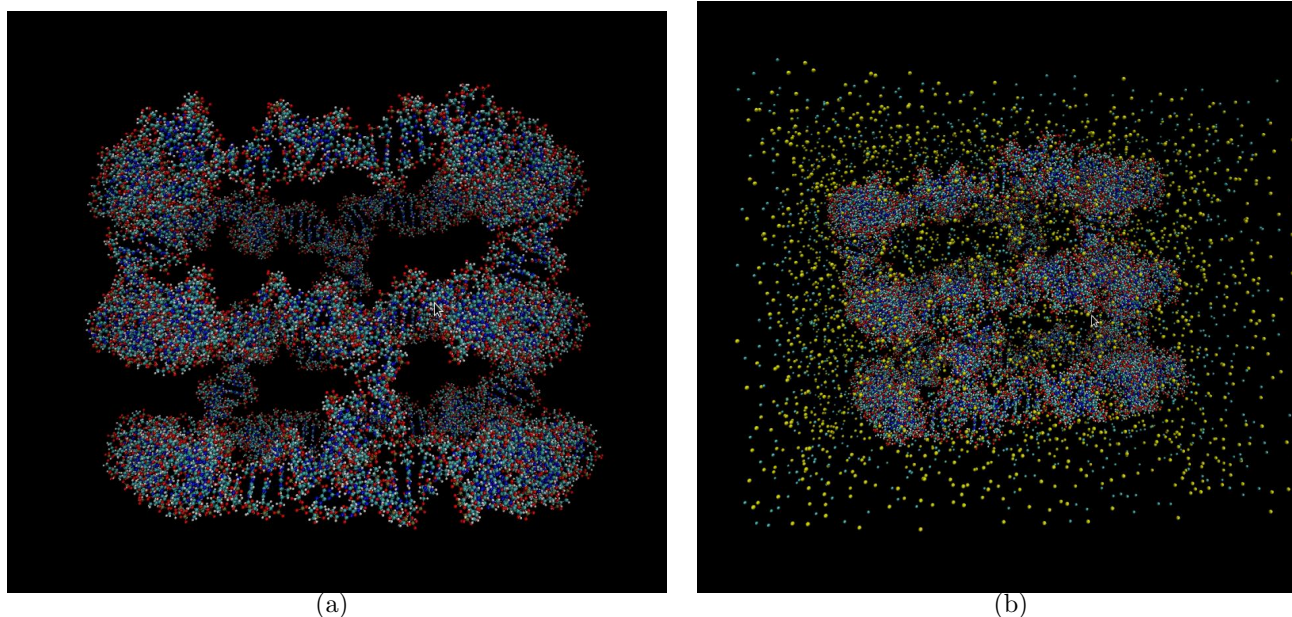
<center>(a)</center><center>(b)</center>

Figure 1. (a) Optimized geometry RNA nanotube modeled by using VMD (b) RNA nanotube in a physiological solution (only the ions around the nanotube are displayed).

3. RESULTS AND DISCUSSION

We used the RNAI/II building blocks to construct the RNA nanotube using molecular dynamics simulation. More details about the construction of the RNA nanoclusters using these RNA building blocks have been provided in our earlier work.[8,9] The sample structures of the optimized geometry of three ring nanotube without water and in a physiological solution are presented in Figure 1(a) and (b) respectively. The six helical segments are constructed from RNAI and RNAII building blocks. We also note that, the tails used to connect the RNA nanorings are the double strand RNAs with the length of 22 nucleotides. Here we present the properties for the RNA nanotube at different concentrations of the salt solution. In particular, the lowest concentration level is characterized by n, where n is the total number of phosphate groups in the nanotube which is ultimately the total number of residues in the system. The next level of the concentration is related to $2n$ i.e the number of $^{23}Na^+$ and $^{35}Cl^-$ has been twice of the number of the ions in the first solution. Here in our particular case the value of n is 924. The variations of energy and temperature with simulation time have been studied for all sets of simulations and the analysis of the results has been done at the production region of the energy plot.

At first, we discuss the results for the ionic distribution around the surface of the tube at a distance of the 5 $\mathring{A}$ at different concentrations, root mean square deviation, radius of gyration, and the hydrogen bonds per base pairs are presented in Figure 2 (a)-(d). From the ionic distribution plot presented in Figure 2(a), we see that the number of ions increases as function of time at the beginning which later becomes consistent at a particular concentration. Furthermore, there is no significant change in the number of $^{23}Na^+$ ions around the surface of the tube as the concentration of the system is doubled. This feature of the ionic distribution function reveals that there is a saturation of the number of ions around the tube and the rest of the ions are uniformly distributed around the tube immersed in the physiological solution . A similar trend has been observed for the $^{35}Cl^-$ ions but the number of ions is significantly smaller in comparison to the number of $^{23}Na^+$ ions indicating the net negative polarity of the surface of the RNA nanocluster as found in our earlier studies.[8,9] The results presented in Figure 2 (c) and (d) for the radius of gyration and the root mean square deviation also show a similar pattern at two different concentrations.

The results for the radial distribution function for the RNA nanotube at different concentrations of the physiological solution are presented in Figure 3. From the radial distribution function plot for Phosphorous-Phosphorous atoms presented in Figure 3 (a), we see that the nature of the distribution is similar at both concentrations. But the peak of the distribution function has been increased slightly with position being at around the same location. The position of the first peak for both plots is around 6.0 $\mathring{A}$. The P-OH2 radial distribution function at different concentrations of the physiological solution has been presented in Figure 3 (b). The peaks observed in the plot show the solvation shell of the water molecule around the
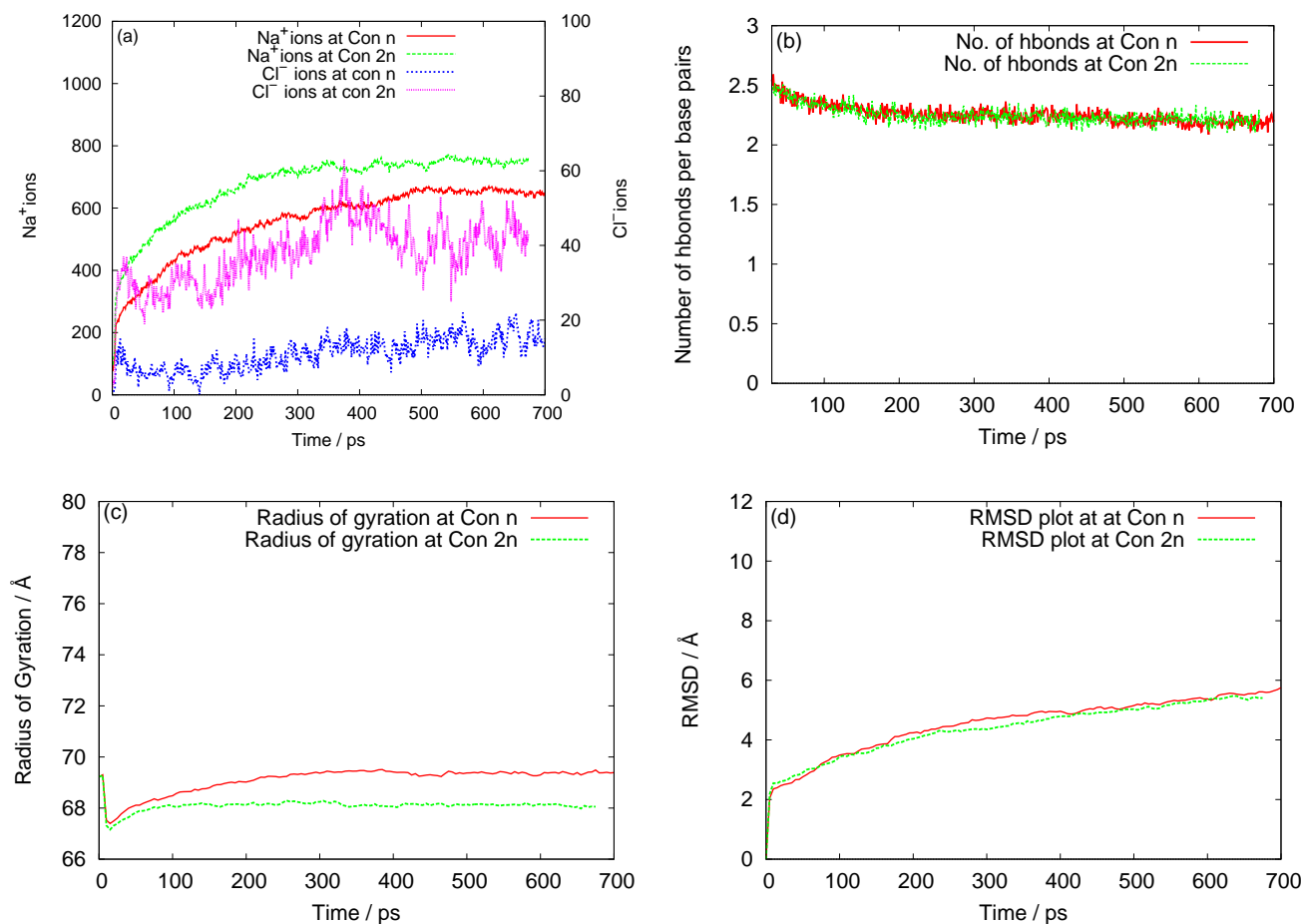
Figure 2. (a) Number of ions with the range of 5 Å (b) Number of bonds per base pairs (c) Radius of gyration and (d) RMSD of 4 ring RNA nanotube obtained from all atom molecular dynamics simulation.

Phosphorous atom. From comparison, we see that the heights of the peaks in the RDF plots are changed by very small amount on going from low to high concentrations of the physiological solution. Note also that the positions of the peaks are not changed on going from low to hight concentrations as found in the case of P-P radial distribution plots. The position of the first peak is found to be at around 4.5 Å.

Finally, the RDF plots for P-Na and P-Cl are presented in Figure 3 (c) and (d). The first peak for the P-Na RDF plot is at 3.5 Å for both concentrations of the physiological solution. This indicates that the most of the sodium ions are around this distance at the end of all-atom MD simulation at two different concentrations. This also gives the information that the results are not dependent on the concentration of the solution. These results are found to be identical to the results obtained in the case of the nanoring as well as to the results for the RNA nanotubes of different sizes at the same concentration.[8,9] Furthermore, from the RDF plot for P-Cl it is clear that the $^{35}Cl^-$ ions are way far from the surface of the RNA nanocluster at both concentrations. The height of the radial distribution function at a particular distance in the RDF plot is proportional to the number of $^{35}Cl^-$ ions around that distance. Therefore, from the plot it is clear that the values of RDF function is initially small and keeps increasing at the beginning and becomes stable after a certain distance. This indicates that there is a very low concentration of $^{35}Cl^-$ ions close to the surface of the RNA nanotube and later on the ions are distributed uniformly inside the simulation box at both concentrations.
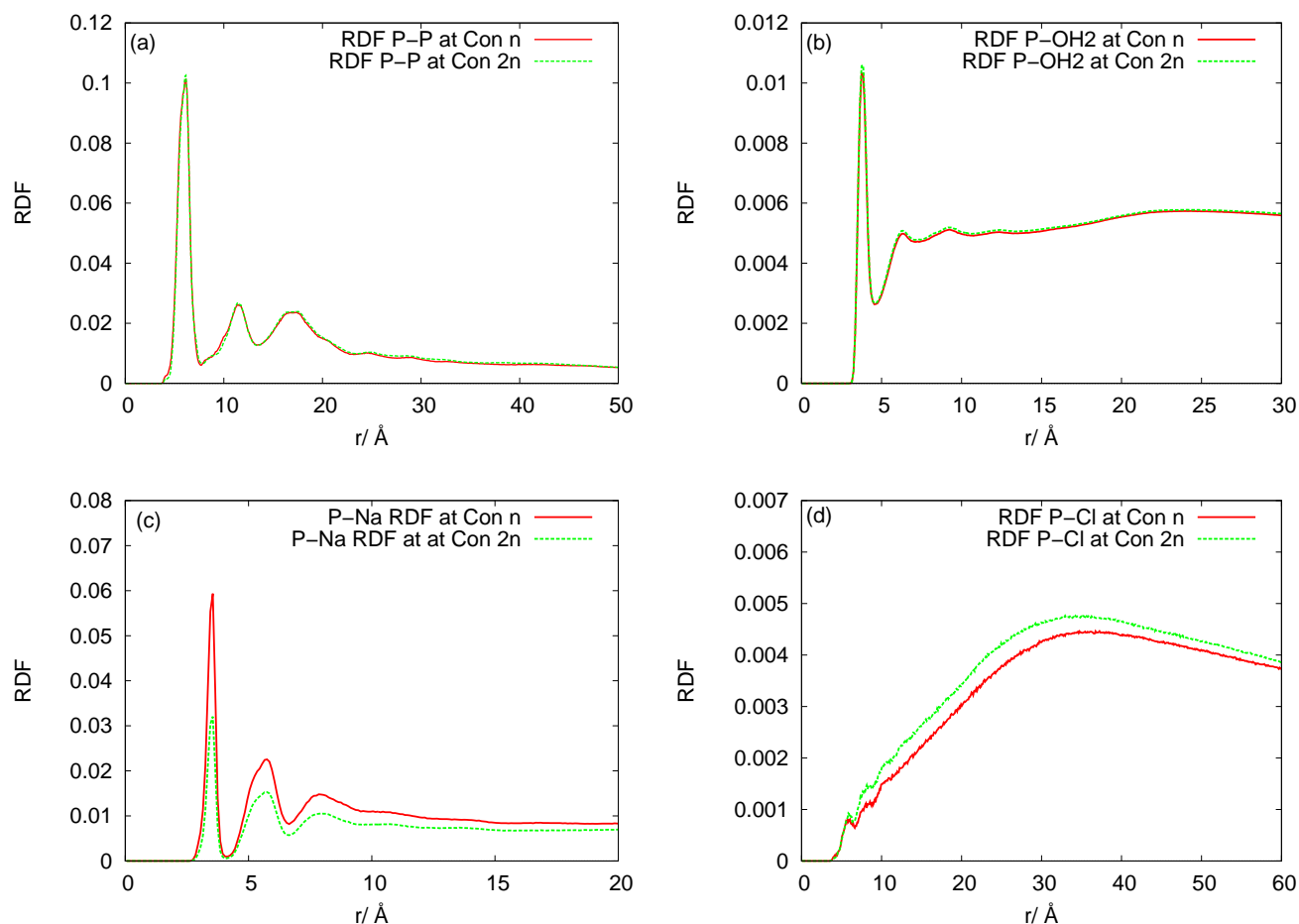
Figure 3. Radial distribution function for 3 ring RNA nanotube (a) P-P (b) P-OH2 (c) P-Na (d) P-Cl.

4. CONCLUSIONS

In this paper we have presented the optimized geometry for the RNA nanotube and calculated the properties such as the ionic distribution, radial distribution function and the root mean square deviation at different concentrations of the physiological solution. The concentration dependence studies will give additional insight into RNA nanocluster properties and assist in further progress of bionanotechnology. In our most recent study,[9] we have analyzed the optimized structures of nanotubes up to the size of 20nm, including all the chemical bonds between different segments. We found that the properties are not sensitive to the size of the nanocluster. Earlier we studied the properties at the same concentration of the physiological solution at two different temperatures. During the construction of the RNA nanotube the individual RNA nanorings were connected via double-helical rings mediated by the bonds between the phosphate group and sugar ring. The newly added bond lengths have been optimized by using algorithms available in NAMD. Then, starting from the nanorings, the results for the RNA nanotubes of different sizes have been discussed in details. Here we presented the analysis which was performed for different concentrations of the physiological solution. We observed that the results are not varying much on going from the low to high concentrations. We have presented our results only for two concentrations. Further insight can be obtained by using our methodology of molecular dynamics simulations for additional sets of concentrations of the physiological solution. From our analysis of the results it is clear that the quality of the results is likely to be improved further by doing the MD simulation for longer time ranges. The studies of properties by using a coarse-grained model that allows us to perform MD simulations for longer ranges of time are currently in progress. These longer time range simulations would better reflect the time range of biological processes, typical for many applications in bionanotechnology. In its turn, these new results could complement our present findings and provide further guidance to experimentalists working in this field.

5. ACKNOWLEDGEMENT

REFERENCES

[1] Sugimoto, N., Nakano, S.-i., Katoh, M., Matsumura, A., Nakamuta, H., Ohmichi, T., Yoneyama, M., and Sasaki, M., "Thermodynamic parameters to predict stability of RNA/DNA hybrid duplexes," *Biochemistry* **34**, 11211–11216 (Sept. 1995).

[2] Guo, P., "The emerging field of RNA nanotechnology," *Nat Nano* **5**, 833–842 (Dec. 2010).

[3] Guo, P., "RNA nanotechnology: Engineering, assembly and applications in detection, gene delivery and therapy," *J Nanosci Nanotechnol* **5**, 1964–1982 (Dec. 2005).

[4] Osada, E., Suzuki, Y., Hidaka, K., Ohno, H., Sugiyama, H., Endo, M., and Saito, H., "Engineering RNAprotein complexes with different shapes for imaging and therapeutic applications," *ACS Nano* **8**, 8130–8140 (Aug. 2014).

[5] Simpson, A. A., Tao, Y., Leiman, P. G., Badasso, M. O., He, Y., Jardine, P. J., Olson, N. H., Morais, M. C., Grimes, S., Anderson, D. L., Baker, T. S., and Rossmann, M. G., "Structure of the bacteriophage 29 DNA packaging motor," *Nature* **408**, 745–750 (Dec. 2000).

[6] Cayrol, B., Nogues, C., Dawid, A., Sagi, I., Silberzan, P., and Isambert, H., "A nanostructure made of a bacterial noncoding RNA," *J. Am. Chem. Soc.* **131**, 17270–17276 (Dec. 2009).

[7] Delebecque, C. J., Lindner, A. B., Silver, P. A., and Aldaye, F. A., "Organization of intracellular reactions with rationally designed RNA assemblies," *Science* **333**, 470–474 (July 2011).

[8] Paliy, M., Melnik, R., and Shapiro, B. A., "Molecular dynamics study of the RNA ring nanostructure: a phenomenon of self-stabilization," *Phys. Biol.* **6**, 046003 (Dec. 2009).

[9] Badu, S. R., Melnik, R., Paliy, M., Prabhakar, S., Sebetci, A., and Shapiro, B. A., "Modeling of RNA nanotubes using molecular dynamics simulation," *Eur Biophys J* **43**, 555–564 (Nov. 2014).

[10] Yingling, Y. G. and Shapiro, B. A., "Computational design of an RNA hexagonal nanoring and an RNA nanotube," *Nano Lett.* **7**, 2328–2334 (Aug. 2007).

[11] Tomizawa, J.-i., "Control of cole 1 plasmid replication: The process of binding of RNA i to the primer transcript," *Cell* **38**, 861–870 (Oct. 1984).

[12] Tomizawa, J.-I., "Control of ColE1 plasmid replication: Binding of RNA i to RNA II and inhibition of primer formation," *Cell* **47**, 89–97 (Oct. 1986).

[13] Lee, A. J. and Crothers, D. M., "The solution structure of an RNA looploop complex: the ColE1 inverted loop sequence," *Structure* **6**, 993–1007 (Aug. 1998).

[14] Vieregg, J., Cheng, W., Bustamante, C., and Tinoco, I., "Measurement of the effect of monovalent cations on RNA hairpin stability," *J. Am. Chem. Soc.* **129**, 14966–14973 (Dec. 2007).

[15] Jaeger, L., Westhof, E., and Leontis, N. B., "TectoRNA: modular assembly units for the construction of RNA nano-objects," *Nucl. Acids Res.* **29**, 455–463 (Jan. 2001). PMID: 11139616.

[16] Kim, T. and Shapiro, B. A., "The role of salt concentration and magnesium binding in HIV-1 subtype-a and subtype-b kissing loop monomer structures," **31**(5), 495–510 (2013). PMID: 22812415.

[17] Hansson, T., Oostenbrink, C., and van Gunsteren, W., "Molecular dynamics simulations," *Current Opinion in Structural Biology* **12**, 190–196 (Apr. 2002).

[18] Lindahl, E. R., "Molecular dynamics simulations," *Methods Mol. Biol.* **443**, 3–23 (2008).

[19] Phillips, J. C., Braun, R., Wang, W., Gumbart, J., Tajkhorshid, E., Villa, E., Chipot, C., Skeel, R. D., Kal, L., and Schulten, K., "Scalable molecular dynamics with NAMD," *J. Comput. Chem* **26**(16), 1781–1802 (2005).

[20] MacKerell, Bashford, D., Bellott, Dunbrack, Evanseck, J. D., Field, M. J., Fischer, S., Gao, J., Guo, H., Ha, S., Joseph-McCarthy, D., Kuchnir, L., Kuczera, K., Lau, F. T. K., Mattos, C., Michnick, S., Ngo, T., Nguyen, D. T., Prodhom, B., Reiher, W. E., Roux, B., Schlenkrich, M., Smith, J. C., Stote, R., Straub, J., Watanabe, M., Wirkiewicz-Kuczera, J., Yin, D., and Karplus, M., "All-atom empirical potential for molecular modeling and dynamics studies of proteins," *J. Phys. Chem. B* **102**, 3586–3616 (Apr. 1998).